Macroscopic and Microscopic Thermodynamic Observations in Swollen Poly(vinyl acetate) Networks

Ferenc Horkay,†,‡ Anne-Marie Hecht,‡ Simon Mallam,‡ Erik Geissler,*,‡ and Adrian R. Rennie§

Laboratoire de Spectrométrie Physique,∥ Université Joseph Fourier de Grenoble, B.P. 87, 38402 St. Martin D'Hères Cedex, France, and Institut Laue Langevin, 156X Centre de Tri, 38042 Grenoble Cedex, France

Received August 6, 1990; Revised Manuscript Received November 29, 1990

ABSTRACT: Thermodynamic and scattering properties of chemically cross-linked poly(vinyl acetate) (PVAc) networks swollen in toluene are investigated and compared with those of the corresponding un-cross-linked polymer solution. The swelling pressure data are described by a two-term equation consisting of a separable elastic and mixing contribution. The mixing term for the gel is smaller than for the solution, but both exhibit a similar concentration dependence. Thermodynamic information is obtained from small-angle neutron and X-ray scattering measurements for both the solution and the gel at different stages of dilution. The scattering signal of the gel is separated into a static and a solution-like part. The latter is compared with the swelling pressure of the gel obtained from the macroscopic osmotic measurements. The agreement found is generally satisfactory, although not perfect.

Introduction

For semidilute solutions of neutral polymers both the osmotic and the scattering properties have been extensively explored.[1-3] It is found that, in the good solvent condition and also in the Θ state, the experimental results can be satisfactorily described by a scaling theory. In spite of the large number of such investigations, few have been devoted to comparing data obtained by complementary macroscopic and microscopic methods. It is known, however, that the osmotic pressure is inversely proportional to the scattering intensity at small angles.

When cross-links are introduced into a polymer array in sufficient number, a gel is formed in which permanent constraints are imprinted on the configurations of the polymer chains. The presence of such constraints reduces the number of configurations accessible to the polymer chains compared with the solution, and the structural and osmotic properties of the resulting network are thereby both modified.

It is our aim here to make two comparisons. First, the macroscopically observed osmotic properties of polymer solutions will be compared with those of the corresponding randomly cross-linked gels; second, these properties will be compared with the thermodynamic information obtained from small-angle X-ray and neutron scattering spectra for both the solutions and the gels. The system investigated here is poly(vinyl acetate)–toluene.

Theoretical Background

Thermodynamic Considerations. The swelling of networks in a solvent is governed by two opposing effects: an osmotic force, due to mixing polymer and solvent molecules, that causes the gel to expand and an elastic force that tends to contract the network and expel the solvent.[4-6] At equilibrium with the pure diluent, the two terms compensate each other in such a way that the osmotic swelling pressure ω becomes zero. In general

$$\omega = \Pi - G \tag{1}$$

Here, Π (mixing pressure) is the osmotic contribution of the cross-linked polymer and G is the elastic modulus of the gel. In classical rubber elasticity theory,[4-6] G, which is identified with the shear modulus, varies with polymer volume fraction φ as

$$G = G_0\varphi^m \tag{2}$$

G_0 is a constant that depends on the given network, and $m = {}^1/_3$.

In the polymer solution theory of Flory and Huggins,[5] the mixing contribution Π is represented by the expression

$$\Pi = -(RT/v_1)[\ln(1-\varphi) + \varphi + \chi\varphi^2] \tag{3}$$

where χ is the polymer–solvent interaction parameter and v_1 is the partial molar volume of the solvent. In contrast, scaling theories of polymer solutions[1,7-9] predict a power law behavior for the concentration dependence of the osmotic pressure in the asymptotic semidilute regime (i.e., $\varphi \ll 1$):

$$\Pi = A_0\varphi^n \tag{4}$$

where $n \approx 9/4$ in a good solvent and $n = 3$ in Θ conditions. The numerical constant A_0 depends on the particular polymer solvent pair. In the following analysis, the swelling pressure will be represented by the expression[10-12]

$$\omega = A_0\varphi^n - G_0\varphi^m \tag{5}$$

where A_0, G_0, n, and m are taken to be free parameters.[13]

Scattering Considerations. The intensity of radiation scattered from a binary solution is governed by the amplitude of the concentration fluctuations, $\langle\Delta\varphi^2\rangle$, which, for a system enjoying full translational freedom of the component molecules, is inversely proportional to the osmotic compressional modulus. Thus, in the case of a polymer solution, the neutron scattering intensity $I(Q)$ is given by

$$I(Q) = a\frac{kT(\rho_p - \rho_s)^2\varphi^2}{K_{os}}S_s(Q) \tag{6}$$

where a is a constant depending on the neutron wavelength and the scattering geometry used, K_{os} ($=\varphi\partial\Pi/\partial\varphi$) is the osmotic compressional modulus, ρ_p and ρ_s are the scattering length densities of the polymer and the solvent respectively, $S_s(Q)$ is the structure factor of the solution, and Q

† On leave of absence from the Department of Colloid Science, Eötvös Loránd University, Budapest, Hungary.
‡ Université Joseph Fourier de Grenoble.
§ Institut Laue Langevin.
∥ CNRS associate laboratory.

0024-9297/91/2224-2896$02.50/0

$= (4\pi/\lambda)\sin(\theta/2)$ is the transfer wave vector for an incident wavelength λ and scattering angle θ. For semidilute solutions, at small values of Q the structure factor can be approximated by a Lorentzian line-shape function

$$S_s(Q) = 1/(1 + Q^2\xi^2) \tag{7}$$

where ξ is the density–density correlation length in the solution.

For gels, the cross-links restrict free movement of the polymer segments, causing the buildup of regions of excess polymer content that appear as permanent departures from uniformity. The mean square amplitude of such static excursions is denoted $\langle\delta\varphi^2\rangle$, and their existence renders eq 6 inadequate as a description of the gel scattering spectrum. The polymer distribution may be viewed as a static structure, with movements of limited amplitude being executed around some mean (or slowly varying) position. Thus the total amplitude of the concentration fluctuations will be approximated by the sum of two parts, a dynamic plus a static part:

$$\langle\Delta\varphi^2\rangle = \langle\Delta\varphi^2\rangle_{dyn} + \langle\delta\varphi^2\rangle \tag{8}$$

For the structure factors of each of these contributions, it has been proposed previously[14] that the dynamic part be represented by a solution-like form analogous to eq 6 with a structure factor of the same type as eq 7. The structure factor of the static component is assumed to have the form $\exp(-Q^s\Xi^s)$, where Ξ is the mean size of the static nonuniformities and s is a positive constant. This expression obeys the requirement of having a finite second moment. The assumption (8) of additivity thus yields for the total scattering intensity

$$I(Q) = a(\rho_p - \rho_s)^2\left[\frac{kT\varphi^2}{M_{os}}\frac{1}{1 + Q^2\xi^2} + f(s)\exp(-Q^s\Xi^s)\right] \tag{9}$$

in which ξ is the correlation length in the solution-like part of the gel. The normalization factor $f(s)$ has the form

$$f(s) = \frac{2\pi^2 s\langle\delta\varphi^2\rangle\Xi^3}{\Gamma(3/s)} \tag{9a}$$

where Γ is the gamma function (cf. Appendix A). In a dynamic scattering experiment, on account of the finite value of G in a gel, the compressional osmotic modulus K_{os} in the solution should be replaced by the longitudinal osmotic modulus in the gel, $M_{os} = K_{os}^g + 4G/3$, where $K_{os}^g = \varphi\partial\omega/\partial\varphi$ and the superscript g refers to the gel.[15] In the absence of information to the contrary, we assume that the macroscopic shear modulus G is also the relevant parameter for the intensity in a static scattering experiment.

Equation 9 has recently been found to be in reasonable agreement with the scattering behavior of end-linked poly(dimethylsiloxane) gels swollen in toluene,[16] when s is equal to 2. This value corresponds to a Gaussian spatial distribution for the nonuniformities in the gel.

Experimental Section

Gel Preparation and Macroscopic Methods. PVAc gels were prepared by acetylation of chemically cross-linked poly(vinyl alcohol) networks using a method described elsewhere.[17,18] Cross-links were introduced into aqueous solutions of polymer concentration 3, 6, 9, and 12% w/w. The cross-linking agent was glutaraldehyde. At each concentration several gel samples were prepared with different molar ratios of monomer units to the molecules of the cross-linking agent. The gels are designated by the code X/Y, where X is the concentration of the polymer at cross-linking in percentage weight fraction and Y is the ratio of monomer units to cross-linker.

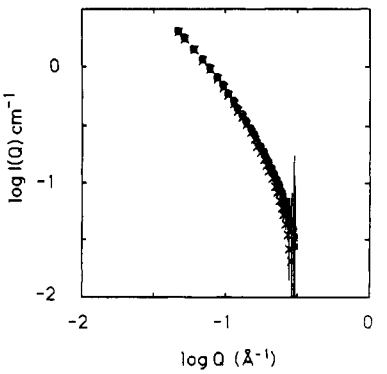

Figure 1. Variation in coherent scattering spectrum of gel 6/50 in the range 0.03 Å^{-1} < Q < 0.3 Å^{-1} generated by substituting different incoherent background samples, using eq 10. Symbols correspond to backgrounds of different protonated toluene content with transmissions: +, T_b = 0.703; X, T_b = 0.779; O, T_b = 0.83; □, T_b = 0.88. Error bars shown are calculated from counting statistics. Sample transmission T_s = 0.82.

The swelling pressure and the shear modulus of gels swollen in toluene were determined at 25 °C as a function of the concentration. Deswelling was induced in the swollen network by surrounding it with PVAc solutions of known toluene activity.[19] The gels were enclosed in dialysis bags to prevent penetration by the polymer molecules.[20]

Shear modulus G data were obtained from uniaxial compression measurements performed at constant volume, in an apparatus described elsewhere.[21] The stress–strain data in the range of deformation ratio $0.7 \le \Lambda < 1$ were evaluated by the Mooney-Rivlin equation, which yielded C_2 equal to zero.

The mixing pressure Π was obtained by analyzing the swelling pressure data in terms of eq 5, where the exponents m and n and the linear coefficients A_0 and G_0 were taken to be free variables. This analysis also yields an independent estimate for the elastic modulus.

Scattering Measurements. The small-angle neutron scattering (SANS) measurements were made on the D11 instrument at the Institut Laue Langevin, Grenoble, using an incident wavelength of 6 Å. The Q range explored was 0.003 Å$^{-1} \le Q \le$ 0.3 Å^{-1}, and counting times of between 20 min and 1 h were used. The ambient temperature during the experiments was 25 ± 1 °C. After radial averaging, the following correction for incoherent background, detector response, and cell window scattering was applied to obtain the coherent scattering signal of the sample:

$$I(Q) = \frac{\left[i_s(Q) - \frac{1 - T_s}{1 - T_b}i_b(Q) - \frac{1}{T_c}\frac{T_s - T_b}{1 - T_b}i_c(Q)\right]}{\left[i_w(Q) - \frac{T_w}{T_c}i_c(Q)\right]}\frac{T_w}{T_s}\frac{d\Sigma_w}{d\Omega} \tag{10}$$

where i_s, i_b, i_c, and i_w are the uncorrected signals from the sample, background, empty cell, and water, respectively, and T_s etc. are the corresponding transmissions normalized with respect to the unimpeded beam (cf. Appendix B). Calibration of the scattered neutron intensity was performed using the signal from a 1-mm-thick water sample in conjunction with the absolute intensity measurements of Ragnetti et al.[22]

The sample cells consisted of 1-mm-thick quartz windows with a 1-mm-thick annular Teflon spacer housing the swollen gel or solution. Deuterated toluene (Janssen) was taken as the solvent throughout, except for the contrast variation measurements, where fixed ratios of protonated and deuterated toluene were used. The background samples consisted of mixtures of protonated and deuterated toluene in proportions chosen to have a transmission factor as close as possible to that of the sample.

Signal correction procedures become important at higher values of Q where the coherent contribution decreases. The robustness of the present data to uncertainties in the incoherent background sample is illustrated in Figure 1. Here $I(Q)$ in the highest Q range is shown for one of the gel samples in the present investigation (gel 6/50, φ = 0.208). The scattering signals recorded from four different backgrounds having relative transmissions

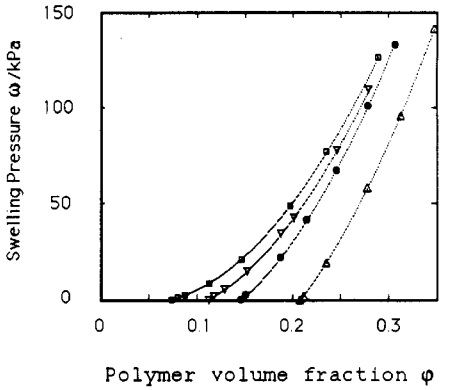

Figure 2. Swelling pressure ω as a function of polymer volume fraction φ for poly(vinyl acetate) networks swollen in toluene. The curves are the least-squares fits to eq 5. Symbols: □, 9/400; ▽, 9/200; ●, 6/50; △, 9/50.

Table I
Parameters of Equation 5 for PVAc Networks Swollen in Toluene at 25 °C

						G (at ϕ_e)/kPa	
sample	A_0/kPa	n	m	G_0/kPa	ϕ_e[a]	swell.	shear
3/50	2171	2.28	0.342	19.7	0.089	8.6	8.9
6/50	2613	2.29	0.331	59.7	0.146	31.6	32.4
6/200	2072	2.22	0.340	17.1	0.078	7.2	6.9
9/50	2481	2.27	0.355	123.6	0.208	70.8	70.3
9/100	2350	2.25	0.336	55.2	0.141	28.6	28.3
9/200	2374	2.27	0.326	33.9	0.112	16.6	16.7
9/400	2273	2.27	0.315	14.2	0.074	6.2	6.3
12/50	3100	2.35	0.383	168.3	0.229	95.7	99.8
12/200	2425	2.26	0.335	50.1	0.133	25.5	25.2

[a] ϕ_e: volume fraction of the polymer in the fully swollen network.

in the range $0.7 \leq T_b \leq 0.9$ were successively taken for $i_b(Q)$ in eq 10. The vertical bars represent the total accumulated error due to counting statistics in the data collection. No background-dependent trend appears in the range up to $Q \leq 0.25$ Å^{-1}, and the consistency among the results is good. Above 0.25 Å^{-1} the data become unreliable in the present experiment, and so are discarded.

The small-angle X-ray scattering (SAXS) measurements were performed on the PVAc–toluene solutions using the D24 instrument at the Laboratoire pour l'Utilisation du Rayonnement Electromagnétique (LURE), Orsay, France. Samples were placed between two mica sheets separated by a 1-mm annular spacer. A 6-cm linear detector with 256-point resolution was used, with a sample–detector distance of 1.2 m. The incident wavelength was 1.608 Å. A toluene sample in the same cell was used for background subtraction, and the resulting difference signal was normalized by the independently measured detector response. In this case, because signal attenuation results from absorption, background subtraction is performed using

$$I(Q) = [i_s(Q)/T_s - i_b(Q)/T_b]/d(Q) \qquad (10a)$$

where $d(Q)$ is the detector response to a uniform γ-ray source. This analysis contrasts with that of eq 10, where attenuation of the coherent signal is the source of the incoherent background.

Results and Discussion

Macroscopic Measurements. In Figure 2 representative swelling pressure data of PVAc gels in toluene are displayed as a function of polymer volume fraction φ. The lines shown are the least-squares fits of the data points to eq 5, and Table I lists the corresponding values of the parameters A_0, n, m, and G_0. The values of n and m are close to those expected theoretically, i.e., 9/4 and 1/3, respectively. In the last two columns of Table I the values of the elastic moduli calculated from the swelling pressure parameters are listed beside those of G obtained by direct mechanical measurement. The agreement between these

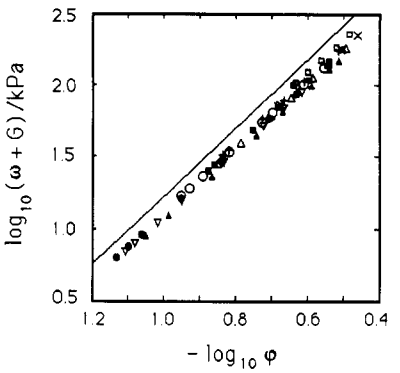

Figure 3. Double-logarithmic representation of mixing pressure $\omega + G$ as a function of polymer volume fraction φ for poly(vinyl acetate)–toluene gels. Continuous line refers to solution of uncross-linked polymer. Different symbols refer to different gel samples.

two sets of data indicates that the same quantity is being measured by the two different techniques and is evidence for the validity of eq 5, i.e., for the separability of the elastic and mixing free energy contributions.

In Figure 3 the mixing pressure for the gels, $\Pi_g = \omega + G$, is compared with Π_s from the solutions, calculated from high-precision osmotic pressure measurements reported by Vink.[19] In the double-logarithmic plot of this figure, it can be seen that both quantities exhibit a similar dependence throughout the concentration range investigated but that the values of Π_s lie systematically below the solution data.

It is reasonable to attribute the difference in the mixing pressure to the structural differences between the gel and the polymer solution: apparently only a reduced fraction of the network polymer exhibits solution-like behavior. In the gel the movements of the segments are hindered by the presence of the cross-links, and the degree of freedom of the polymer chains is accordingly smaller than in the solution. It is also likely that the local polymer concentration is increased in the vicinity of the network junctions.

These macroscopic observations thus favor an expression for the free energy of the gel consisting of an elastic and a mixing term that are separable. The concentration dependence of the mixing term of the gel is closely similar to that of the solution.

Microscopic Measurements. An important precondition for straightforward interpretation of the scattering measurements is that the gels be chemically uniform. Neutron scattering is sensitive not only to the geometrical structure, through the structure factor $S(Q)$, but also the chemical composition of the sample, through the difference in scattering length densities ρ_p and ρ_s of polymer and solvent. Contrast variation[23,24] provides an indicator of any chemical inhomogeneity that may be present in the sample.

In contrast variation the scattering length density ρ_s is changed by varying the proportion D of deuterated molecules in the solvent. From eqs 6 and 9, it follows that if the plot of $(I(Q))^{1/2}$ versus D is linear, then only one scattering length density ρ_p contributes to the signal; i.e., the system is chemically homogeneous in the range of momentum transfer Q scanned. Figures 4 shows plots of $(I(Q))^{1/2}$ versus D, the deuterated toluene content of the solvent, for identical PVAc gels at different values of Q in the range 0.0036 Å$^{-1} \leq Q \leq 0.09$ Å^{-1}. The straight lines shown are the least-squares fits to the data points at each Q value for the separate spectra. At the two sample–detector distances, 4 and 15 m, the spectra give rise to a family of straight lines crossing the zero intensity axis at

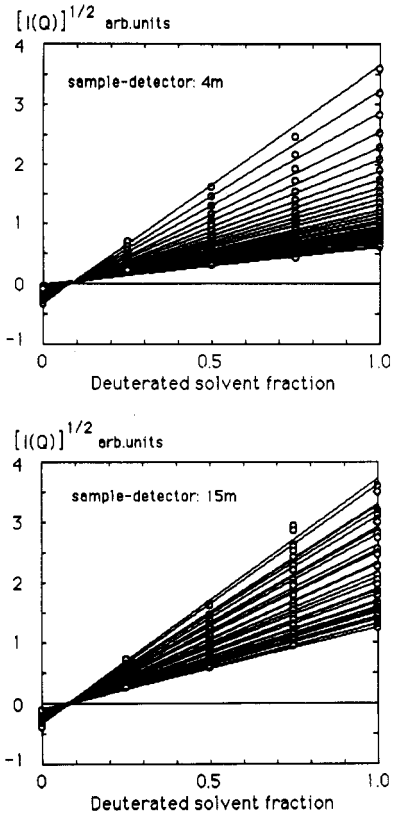

Figure 4. Square root of neutron scattering intensity $(I(Q))^{1/2}$ versus D, the deuterated toluene content of the solvent, for poly(vinyl acetate) networks swollen in toluene. Sample–detector distance: 4 m (top, 0.014 Å^{-1} ≤ Q ≤ 0.1 Å^{-1}); 15 m (bottom, 0.004 Å^{-1} ≤ Q ≤ 0.02 Å^{-1}). Continuous straight lines are least-squares fits through data points with the same Q value.

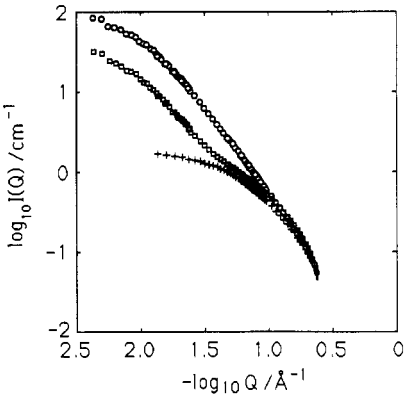

Figure 5. Double-logarithmic representation of the neutron scattering intensity $I(Q)$ as a function of scattering wave vector Q for poly(vinyl acetate)–toluene gel 6/50 at two stages of swelling. ○, Fully swollen gel (φ = 0.146); □, partially deswollen gel (φ = 0.315); +, polymer solution (φ = 0.114).

D = 0.075. From the scattering properties of toluene, this matching point corresponds to a scattering length density of $\rho_p = 1.29 \times 10^8$ cm^{-2}, in excellent agreement with the value of ρ_p calculated from the scattering lengths of the component nuclei of PVAc.[25] It is concluded that on the length scales investigated here, the PVAc gels can be considered as being chemically homogeneous networks of the same composition as the solutions. In other words, neither chemical modifications of the network due to cross-links nor the presence of residual hydroxyl groups are detected in the neutron scattering spectra.

In Figure 5 the scattering spectra of one of the PVAc gels (6/50), obtained at two different degrees of swelling in toluene (φ = 0.146 and 0.315), are compared with that

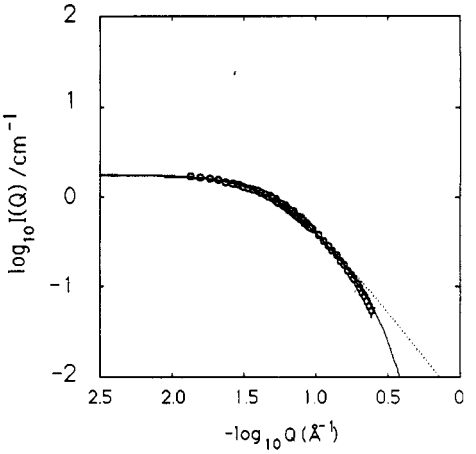

Figure 6. Double-logarithmic plot of the scattering intensity $I(Q)$ as a function of scattering wave vector Q for poly(vinyl acetate) solution at φ = 0.114. The dotted line through the data points is the Lorentzian fit to the low-Q part of the spectrum. The continuous line shows the fit of eq 6 with the form factor of eq 11 to the experimental points.

of a solution (φ = 0.114). At small Q it can be seen that the difference between the gel and the solution spectra is substantial, the scattering signal from the gel greatly exceeding that of the solution. This is in agreement with the expectation that the nonuniformities contribute to the scattering spectrum principally in the low-Q range because of their relatively large size. It is also apparent that in the low-Q region of the spectra the intensity of the gel signal is higher when the swelling degree is higher. At higher Q, the difference between the solution and the gel decreases. A feature of these particular gel spectra is the extended high-Q range of overlap between the intensities of the swollen and the deswollen sample, instead of the more customary crossover observed in other systems.[16]

Figure 6 displays the least-squares fit of eq 6 to the SANS data from the solution. The scattering properties are satisfactorily described by the Lorentzian form factor given in eq 7 (dotted line) for the lower range of Q. At higher Q values, however, the observed intensity consistently falls below the Lorentzian curve. In view of the discussion in the experimental section about the robustness of the data treatment, this drop in intensity does not seem to be an artifact.

In this higher Q region several competing physical effects occur, due to chain stiffness, excluded-volume interactions, and finite chain radius.[26] At the relatively high concentrations investigated here, the effect of the short-range geometry of the chain on the scattering spectrum becomes more pronounced, and consequently the chain radius is expected to be responsible for a decrease in scattering intensity at high Q. We make the crude approximation that on this small scale the polymer behaves as a wormlike chain[27] of radius r_c, whose scattering spectrum is

$$I'(Q) \propto (1/Q) \exp(-Q^2 r_c^2/2) \qquad (11)$$

Combining eq 11 with the line-shape function eq 7 yields the form factor

$$S_s(Q) = \left[\frac{1 + r_c Q/2^{1/2}}{1 + Q^2\xi^2}\right] \exp\left(-\frac{r_c^2 Q^2}{2}\right) \qquad (12)$$

Figure 6 shows the fit of the form factor given by eq 12 to the spectra (continuous line), with a value of r_c = 5 Å. This value is close to the radius of the chain estimated from the density of the dry polymer (ca. 4 Å). Changing the fitting formula from eq 7 to eq 12 does not alter the

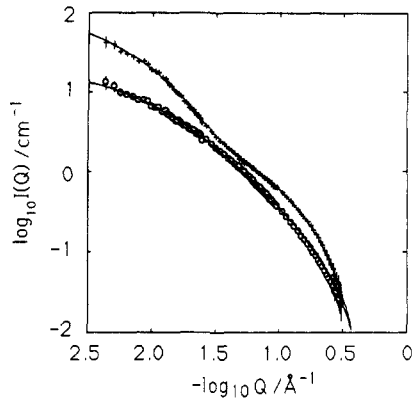

Figure 7. Neutron scattering spectra of poly(vinyl acetate)–toluene gels. The continuous lines through the data points are calculated from eq 12 with the parameters given in Table II. Symbols: ○, gel 9/400 at $\varphi = 0.074$ (fully swollen state); +, gel 6/50 at $\varphi = 0.270$.

value found for the correlation length ξ, but it does allow the range of useful data to be extended to higher Q values. Note that eq 12 loses its physical significance for $Qr_c \gtrsim 1.5$ where the slope in the double-logarithmic representation exceeds −4.

For the gels, a form factor similar to that of the solutions (eq 12) will be assumed, in addition to the static component described in eq 9. This gives

$$I(Q) = a(\rho_p - \rho_s)^2\left[\frac{kT\varphi^2}{M_{os}}S_s(Q) + f(s)\exp\{-(Q\Xi)^s\}\right] = I_1 S_s(Q) + I_2\exp\{-(Q\Xi)^s\} \quad (13)$$

where I_1 and I_2 are constants and $S_s(Q)$ is given by eq 12.

Since the geometrical properties of the constituent monomers are unaffected by the cross-links, r_c should be the same for the gel as for the solution. As seen in Figure 5, the overall shape of the scattering curves changes with degree of swelling. Satisfactory fits to the shape could be obtained only in the vicinity of $s = 0.7$, i.e., considerably lower than for a Gaussian spatial distribution of nonuniformities ($s = 2$). Higher and lower values of s yielded notably poorer fits in the general shape of the curves. This finding is in agreement with the expected broad spectrum of nonuniformities in randomly cross-linked gels. For networks obtained by percolation processes, the spatial distribution of the nonuniformities is not expected to be Gaussian either but instead to be also much broader.[28,29]

For the present gels, the distribution of the polymer is further perturbed by the primary structure of the poly(vinyl alcohol) solutions from which they are prepared. It has been demonstrated that the poly(vinyl alcohol) chains in aqueous solutions are clustered due to the presence of hydrogen bonds.[30,31] All these effects are expected to lead to a value of the exponent s smaller than 2, in accordance with the result of the present investigation.

In the fitting procedure, r_c and s were taken to be fixed, as stated above. The initial value of ξ was chosen to be close to the correlation length of the corresponding solution. For physically meaningful results, the best fit with $\Xi > \xi$ was selected. Figure 7 displays the resulting fits of eq 13 to the data for one deswollen and one fully swollen sample. Over the Q range investigated, the agreement is reasonable in spite of the difference between the shapes of the spectra. The fitting parameters thus calculated are listed in Table II.

The behavior of the static contribution to the scattering spectra is in qualitative agreement with expectations. Figure 5 clearly shows that the intensity of this contribution

Table II
Scattering Parameters[a] from PVAc Networks and Solutions in Toluene at 25 °C

sample	ϕ	I_1/cm^{-1} [b]	I_2/cm^{-1} [b]	ξ/Å	Ξ/Å	$\langle\delta\phi^2\rangle/10^{-3}$
6/50	0.146	1.58	223	15	215	7.5
	0.208	1.74	166	15	236	4.2
	0.270	1.59	131	15	274	2.1
	0.315	1.58	106	17	295	1.4
9/400	0.074	1.14	22	18	158	1.9
solution	0.114	1.76		18		
	0.212	1.18		12		

[a] Calculated with $s = 0.7$. [b] Intensities calibrated[22] with respect to 1 mmH_2O for an incident neutron wavelength of 6 Å.

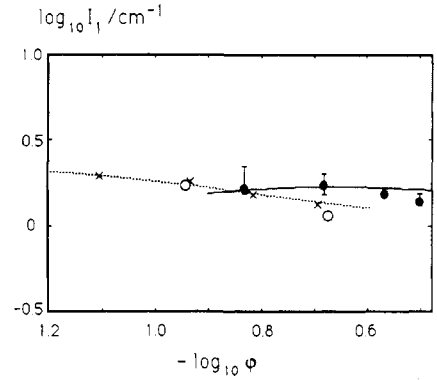

Figure 8. Double-logarithmic plot of the intensity I_1 as a function of the polymer volume fraction φ for poly(vinyl acetate)–toluene gel 6/50 (●) and for solutions (SANS data, x; SAXS data, ○). The continuous curve shows the variation of the intensity calculated from the swelling pressure of the gel and the broken line that from the osmotic pressure of the solution.

decreases at higher gel concentration: the calculated values of the mean square amplitude of the static concentration fluctuations $\langle\delta\varphi^2\rangle$ (Table II) decrease with diminishing swelling degree. That is, as the overall polymer content increases, concentration differences between various parts of the network tend to vanish. Simultaneously, the characteristic size Ξ of the distribution increases. This effect may be the consequence of clustering of nonuniform zones that are spatially separated in the fully swollen network.

From Table II it can also be seen that the parameter ξ hardly varies as a function of gel swelling. This unexpected result reflects the fact that the neutron scattering line shapes at high Q values are very similar (Figure 5). For polymer solutions in a good solvent,[1] the correlation length varies as $\varphi^{-3/4}$. For gels, however, such a simple power law behavior is not altogether appropriate due to the finite elasticity. In the present case, however, the elastic modulus is insufficient to explain the observed invariance of ξ.

In Figure 8 the intensity of the solution-like component of the gel signal (filled circles), i.e.

$$I_1 = a(\rho_p - \rho_s)^2 kT\varphi^2/M_{os} \quad (14)$$

is compared with that of the solution (open circles and crosses). The open circles denote small-angle neutron scattering data, while small-angle X-ray scattering measurements are represented by crosses. The latter data are normalized by a constant factor to align them with the absolute intensities of the SANS measurements. It can be seen from Figure 8 that the intensity of the solution-like component of the gel signal slightly exceeds that of the solution itself. The error bars displayed show the range of I_1 for which good quality fits were obtained.

Comparison between Macroscopic and Microscopic Properties. We now turn to the comparison of the osmotic

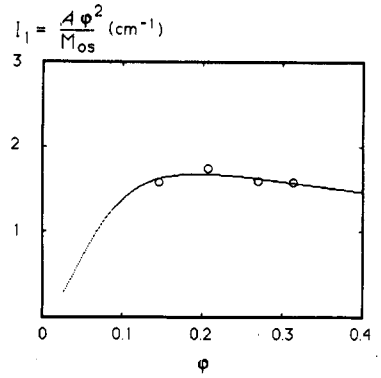

Figure 9. Least-squares fit to eq 13 of the experimental values of $A\varphi^2/I_L(0)$ for poly(vinyl acetate) gel 6/50 at various degrees of swelling in toluene. The constant $A = 0.772 \times 10^6$ kPa·m^{-1} is defined by eq 14.

properties of the PVAc solutions and gels, measured by macroscopic and scattering techniques, respectively.

The broken line in Figure 8 is the theoretical scattering intensity for PVAc–toluene solutions, calculated from the osmotic pressure data of Vink. The normalization factor of eq 6

$$A = a(\rho_p - \rho_s)^2 kT = 0.772 \times 10^6 \text{ kPa·m}^{-1} \qquad (15)$$

is evaluated from the neutron scattering spectrum of water,[22] together with the known scattering densities ρ_p and ρ_s for PVAc and deuterated toluene (1.2904×10^{14} m^{-2} and 5.63×10^{14} m^{-2}, respectively). The experimentally observed absolute scattering intensities for the solutions lie along the calculated curve, demonstrating that for the solutions both the macroscopic and the microscopic techniques probe the same thermodynamic response.

The agreement found for semidilute solutions is an incitement to extend the analysis to swollen gels. As noted above, both the osmotic and the scattering evidence suggest a solution-like component in the swollen network. The data listed in Table I allows the value of M_{os} to be calculated and hence, using eqs 14 and 15, the intensity can be obtained. The solid line in Figure 8 shows the calculated dependence of I_1 on polymer volume fraction for gel 6/50. The theoretical curve lies close to the experimentally observed intensities (filled circles).

The intensity of the thermodynamically active component of the gel signal, I_1, combined with eq 5, provides an independent determination of the parameters A_0, n, m, and G_0 for the gel. The fit to the experimental values of I_1 in gel 6/50 at different stages of deswelling is shown in Figure 9. In the nonlinear least-squares fit applied here m was taken to be equal to $^1/_3$. The resulting best fit to the data points is found for

$$A_0 = 3035 \text{ kPa} \qquad n = 2.42 \qquad G_0 = 61 \text{ kPa} \qquad (16)$$

These values are close to those derived from the macroscopic swelling pressure observations on the same gel (second line in Table I). Note, however, that the error bars displayed in Figure 8 arising from the decomposition procedure lead principally to an uncertainty in G_0. The value of G_0 stated in eq 16 should probably be regarded as an upper limit.

Consistency between macroscopic and microscopic results requires the longitudinal osmotic modulus determined from swelling pressure and shear modulus measurements to be compared with that obtained from the neutron scattering intensities. In Figure 10 M_{os} ($=\varphi\partial\omega/\partial\varphi + 4G/3$) from macroscopic osmotic and mechanical observations is plotted as a function of φ for gel 6/50,

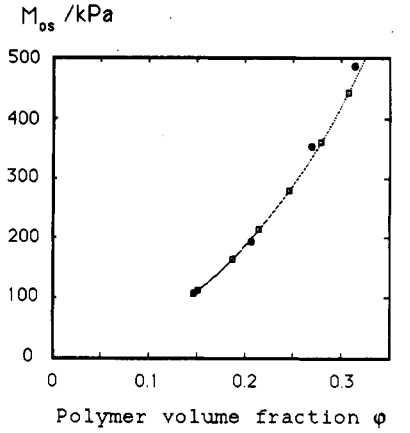

Figure 10. Longitudinal osmotic modulus M_{os} as a function of polymer volume fraction φ for poly(vinyl acetate) gel 6/50 swollen in toluene. □, $M_{os} = \varphi\partial\omega/\partial\varphi + 4G/3$ obtained from independent swelling pressure and shear modulus measurements; ●, M_{os} calculated from scattering intensity data. Curve shows least-squares fit to data points with parameters displayed in Table I.

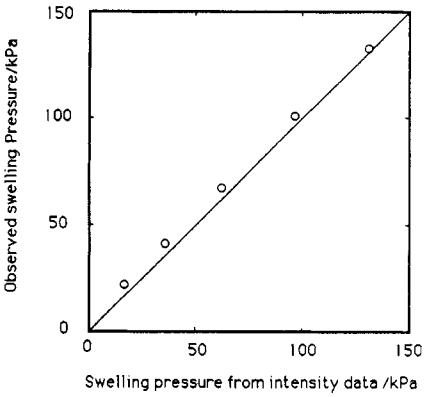

Figure 11. Measured swelling pressure of poly(vinyl acetate)–toluene gel 6/50, plotted as a function of the swelling pressure calculated from the scattering intensity. For the calculation the parameters of eq 16 were used.

together with the values of M_{os} from neutron scattering measurements. In view of the numerous possible sources of error in the separation procedure, the agreement found appears to be acceptable.

In Figure 11 the experimental values of ω for gel 6/50 are plotted against $A_0\varphi^n - G_0\varphi^{1/3}$, using the values for A_0, n, and G_0 from the intensity fit. The resulting points lie close to the theoretical straight line of unit slope through the origin.

Conclusions

We present experimental results on the osmotic and scattering properties of PVAc networks swollen in toluene. It is found that the swelling pressure of the gels is described by a two-term equation containing an elastic and a mixing contribution. The concentration dependence of the mixing pressure in the swollen cross-linked polymer is similar to, but smaller than, that of the osmotic pressure of the solution of the same polymer.

The small-angle neutron scattering spectra of the gels are separated into a solution-like part and a static part. Independent osmotic and swelling pressure measurements are used to test the decomposition procedure. It is found that the thermodynamic information of the gel is contained principally in the solution-like component of the scattering signal. The swelling pressure data obtained from macroscopic osmotic observations are consistent with those derived from the scattering intensity. It is concluded that

the thermodynamic responses probed by the two different experimental methods employed here are indistinguishable within the experimental error.

Acknowledgment. F.H. acknowledges the tenure of a Visiting Professorship at the Joseph Fourier University, Grenoble. This work is part of a joint CNRS–Hungarian Academy of Sciences project. We are grateful to the Institut Laue Langevin for beam time on the D11 instrument and to LURE for access to the D24 beam line. We are particularly grateful to J. P. Benoit for his invaluable help with the X-ray scattering measurements.

Appendix A

The factor $f(s)$ in eq 9 can be found from the condition of invariance of the second moment M_2 of the static scattering function. The relation between the mean-square amplitude of the static concentration fluctuations $\langle\delta\varphi^2\rangle$ and M_2 for a sample of unit volume is[32]

$$M_2 = 2\pi^2\langle\delta\varphi^2\rangle \tag{A1}$$

The form of the static scattering intensity in eq 9 gives

$$M_2 = \int_0^\infty Q^2 f(s)\exp[-(Q\Xi)^s]\,dQ = \frac{\Gamma(3/s)}{s\Xi^3}f(s) \tag{A2}$$

where $\Gamma(x)$ is the gamma function. Combining (A1) and (A2) yields

$$f(s) = \frac{2\pi^2 s\langle\delta\varphi^2\rangle\Xi^3}{\Gamma(3/s)} \tag{A3}$$

Appendix B

The formula for background subtraction used for the present data evaluation is obtained under the following assumptions: (1) The samples are sufficiently thin for multiple scattering to be small. (2) Attenuation of the primary beam in the neutron transmission measurements is due to incoherent scattering, i.e., not absorption or small-angle coherent scattering. This implies that the incoherent scattering signal received at the detector is proportional to $1 - T$, where T is the transmission factor of the sample being examined. (3) The coherent scattering signal from the sample, I_{coh}, is attenuated in its passage through the sample by the transmission factor T_s, in the usual way. (4) The observable scattering from the cell windows is confined almost entirely to very small angles; i.e., it is coherent. The incoherent part of the cell scattering is too weak and spread over too wide a solid angle to make any significant contribution to the total incoherent background.

It follows that the raw spectra from sample, background, and empty cell are respectively

$$i_s = T_s I_{coh} + (1 - T_s)I_{inc} + T_s I_{cell} \tag{B1}$$

$$i_b = (1 - T_b)I_{inc} + T_b I_{cell} \tag{B2}$$

$$i_c = T_c I_{cell} \tag{B3}$$

where I_{cell} is the unnormalized specific coherent scattering intensity from the cell and I_{coh} and I_{inc} are respectively the coherent and incoherent signals from the substance investigated. Elimination of I_{cell} and I_{inc} gives for the unnormalized coherent signal from the sample alone

$$I_{coh} = \frac{1}{T_s}\left[i_s - \frac{1 - T_s}{1 - T_b}i_b - \frac{1}{T_c}\frac{T_s - T_b}{1 - T_b}i_c\right] \tag{B4}$$

Normalization of I_{coh} for detector efficiency using the signal from the standard water sample gives eq 10.

Note Added in Proof. In general, cell windows also scatter incoherently, giving rise to an additional term $(1 - T_c)I_{inc}$ in eq B3. The full expression for the normalized coherent scattering signal then becomes

$$I(Q) = \frac{\left[i_s(Q) - \frac{T_c - T_s}{T_c - T_b}i_b(Q) - \frac{T_s - T_b}{T_c - T_b}i_c(Q)\right]}{\left[i_w(Q) - \frac{T_w}{T_c}i_c(Q)\right]}\frac{T_w}{T_s}\frac{d\Sigma_w}{d\Omega} \tag{10'}$$

which replaces eq 10 in the text. For cell windows with high transmissions ($T_c \geq 0.95$ here), however, eqs 10 and 10a become indistinguishable.

References and Notes

(1) Daoud, M.; Cotton, J. P.; Farnoux, B.; Jannink, G.; Sarma, G.; Benoit, H.; Duplessix, R.; Picot, C.; de Gennes, P.-G. *Macromolecules* **1975**, *8*, 804.
(2) Cotton, J. P.; Nierlich, M.; Boué, F.; Daoud, M.; Farnoux, B.; Jannink, J.; Duplessix, R.; Picot, C. *J. Chem. Phys.* **1976**, *65*, 1101.
(3) Nicolai, T.; Brown, W. *Macromolecules* **1990**, *23*, 3150.
(4) James, H. M.; Guth, E. J. *J. Chem. Phys.* **1943**, *11*, 455.
(5) Flory, P. J. *Principles of Polymer Chemistry*; Cornell: Ithaca, NY, 1953.
(6) Treloar, L. R. G. *The Physics of Rubber Elasticity*, 3rd ed.; Clarendon: Oxford, 1975.
(7) de Gennes, P.-G. *Scaling Concepts in Polymer Physics*; Cornell: Ithaca, NY, 1979.
(8) Muthukumar, M.; Edwards, S. F. *J. Chem. Phys.* **1982**, *76*, 2720.
(9) Muthukumar, M. *J. Chem. Phys.* **1986**, *85*, 4722.
(10) Flory, P. J. *Ind. Eng. Chem.* **1946**, *38*, 417.
(11) Ball, R. C.; Edwards, S. F. *Macromolecules* **1980**, *13*, 748.
(12) Bastide, J.; Candau, S.; Leibler, L. *Macromolecules* **1981**, *14*, 719.
(13) Horkay, F.; Geissler, E.; Hecht, A. M.; Zrinyi, M. *Macromolecules* **1988**, *21*, 2589.
(14) Mallam, S.; Hecht, A. M.; Geissler, E.; Pruvost, P. *J. Chem. Phys.* **1989**, *91*, 6447.
(15) Tanaka, T.; Hocker, L. O.; Benedek, G. B. *J. Chem. Phys.* **1973**, *59*, 5151.
(16) Mallam, S.; Horkay, F.; Hecht, A. M.; Rennie, A. R.; Geissler, E. *Macromolecules* **1991**, *24*, 543.
(17) Horkay, F.; Nagy, M.; Zrinyi, M. *Acta Chim. Acad. Sci. Hung.* **1981**, *108*, 287.
(18) Horkay, F.; Zrinyi, M. *Macromolecules* **1982**, *15*, 1306.
(19) Vink, H. *Eur. Polym. J.* **1974**, *10*, 149.
(20) Nagy, M.; Horkay, F. *Acta Chim. Acad. Sci. Hung.* **1980**, *104*, 49.
(21) Horkay, F.; Nagy, M.; Zrinyi, M. *Acta Chim. Acad. Sci. Hung.* **1980**, *103*, 387.
(22) Ragnetti, M.; Geiser, D.; Höcker, H.; Oberthür, R. C. *Makromol. Chem.* **1985**, *186*, 1701.
(23) Jacrot, B. *Rep. Prog. Phys.* **1976**, *39*, 911.
(24) Stuhrman, H. B. In *Small Angle X-ray Scattering*; Glatter, O., Kratky, O., Eds.; Academic Press: London, 1982.
(25) Lovesey, S. W. *Theory of Neutron Scattering from Condensed Matter*; Clarendon: Oxford 1984.
(26) Rawiso, M.; Duplessix, R.; Picot, C. *Macromolecules* **1987**, *20*, 631.
(27) Kirste, R. G.; Oberthür, R. C. In *Small Angle X-ray Scattering*; Glatter, O., Kratky, O., Eds.; Academic Press: London, 1982.
(28) Bastide, J.; Leibler, L. *Macromolecles* **1988**, *21*, 2647.
(29) Bastide, J.; Leibler, L.; Prost, J. *Macromolecules* **1990**, *23*, 1821.
(30) Wu, W.; Shibayama, M.; Roy, S.; Kurokawa, H.; Coyne, L. D.; Nomura, S.; Stein, R. S. *Macromolecules* **1990**, *23*, 2245.
(31) Fang, L.; Brown, W. *Macromolecules* **1990**, *23*, 3284.
(32) Porod, G. In *Small Angle X-ray Scattering*; Glatter, O., Kratky, O., Eds.; Academic Press: London, 1982.